Imaging Fully Hydrated Whole Cells by Coherent X-Ray Diffraction Microscopy

Daewoong Nam,[1,2] Jaehyun Park,[1] Marcus Gallagher-Jones,[1,3] Sangsoo Kim,[1] Sunam Kim,[1] Yoshiki Kohmura,[1] Hisashi Naitow,[1] Naoki Kunishima,[1] Takashi Yoshida,[4] Tetsuya Ishikawa,[1] and Changyong Song[1,*]

[1]*RIKEN SPring-8 Center, 1-1-1 Kouto, Sayo, Hyogo 679-5148, Japan*

[2]*Department of Physics, Pohang University of Science and Technology, Pohang 790-784, Korea*

[3]*Institute of Integrative Biology, University of Liverpool, Liverpool L69 7ZB, United Kingdom*

[4]*Division of Applied Biosciences, Graduate School of Agriculture, Kyoto University, Kitashirakawa Oiwake-cho, Sakyo-ku, Kyoto 606-8502, Japan*

(Received 19 May 2012; published 28 February 2013)

Nanoscale imaging of biological specimens in their native condition is of long-standing interest, in particular with direct, high resolution views of internal structures of intact specimens, though as yet progress has been limited. Here we introduce wet coherent x-ray diffraction microscopy capable of imaging fully hydrated and unstained biological specimens. Whole cell morphologies and internal structures better than 25 nm can be clearly visualized without contrast degradation.

DOI: 10.1103/PhysRevLett.110.098103 PACS numbers: 87.64.Bx, 42.30.Rx, 87.59.−e

The invention of compound microscopes, pioneered by A. v. Leeuwenhoek in the late 17th century, and subsequent developments to investigate biological specimens have drastically expanded our understanding of microsystems by providing views into structural details far beyond those perceivable by the human eye. The tremendous interest in unveiling ultrastructures by introducing new imaging methodologies with improved resolution and functions has not dwindled since then [1]. Progress toward high-resolution microscopy has not only deepened our understanding, but also invoked keen interest in imaging specimens at a condition closer to their physiological state. Cryogenic preservation of biological specimens has been adopted widely as a good proximity to preserving the native state. It, however, is accompanied by stringent sample treatments that can lead to unwanted structural alterations [2].

Realizing that most biological systems exist in a hydrated environment, imaging specimens under full hydration is undoubtedly ideal. Optical microscopy has routinely imaged biological specimens in solution, but image resolution usually remains on a cellular scale. Superresolution techniques have improved this to better than 100 nm, but elaborate sample handling is necessary [3–6]. Moreover, acquired images often visualize only local portions of a whole specimen where fluorescent dyes are located. Developments in electron microscopy to observe whole, hydrated cells with a nanoscale image resolution have been noteworthy [7,8]. Restrictions on sample conditions and degraded image contrast in solution, however, remain a major obstacle for general applications in bioimaging.

The shorter wavelength of x rays holds the promise of higher resolution, introducing various imaging modalities [9]. Differential attenuation of x rays in specimens allows absorption contrast microscopy with either lens or contact registry [10]. Techniques contingent on the phase contrast of specimens such as Zernike phase contrast, holography, Talbot interferometry, etc., have been actively developed, showing good contrast even for low Z materials [11].

Here we introduce a newly developed wet coherent diffraction imaging (wet-CDI) technique capable of imaging fully hydrated, unstained, whole cells. The CDI technique has inherent advantages essential for imaging specimens in solution. Images are acquired by inverting the coherent diffraction patterns recorded finer than the Nyquist sampling frequency with the phases retrieved via numerical iterations [12]. As the diffraction patterns are invariant for any translational sample drift under a plane wave incidence, CDI provides the ultimate imaging stability, critical for high resolution in solution. The straightforward setting in CDI, with no requirement for lens or extrinsic sample treatment, has rapidly expanded applications to biological specimens and nanostructured materials [12–14]. Excellent image contrast is noteworthy in CDI as demonstrated by imaging single, unstained viral particles [15,16]. The image contrast in CDI is not limited by the absorption, but being further enhanced by the phase difference of x rays while interacting with specimens. This facilitates robust high contrast imaging for a wide range of x-ray energies and better addresses its advantage in imaging hydrated specimens compared with lens based electron or x-ray microscopy [8,9,17–19].

To establish the wet-CDI technique, we have developed two key components: a hydrated specimen holder and a helium ambiance x-ray diffraction microscope. The schematics of the diffraction microscope are shown in Fig. 1. The hydrated specimen holder is made of two Si_3N_4 membranes with 5×5 arrays of 30 nm thin windows (Silson Ltd.). Cells were dispersed onto the windows along with a buffer solution, and were sealed up using another membrane, preserving the specimens in a fully hydrated

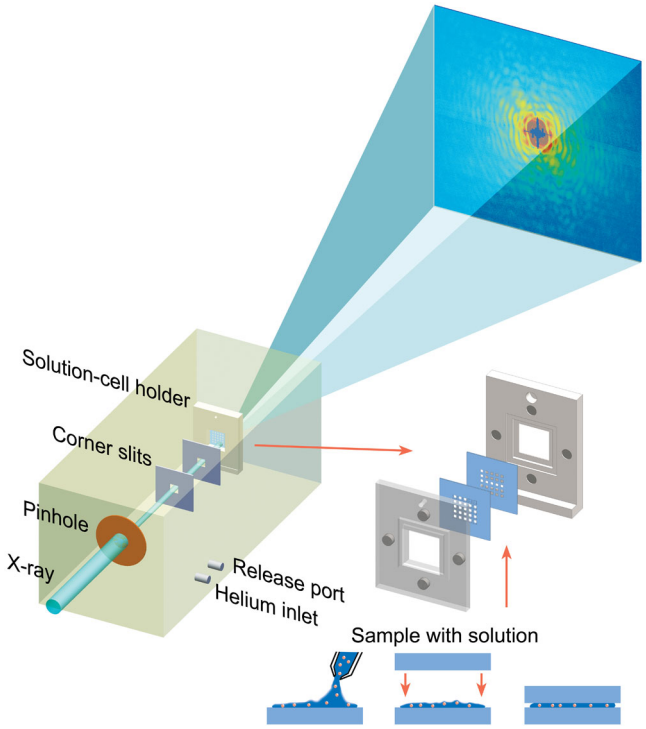

FIG. 1 (color online). Imaging hydrated specimens in wet CDI. Cells suspended in buffer solution are preserved between two membranes. The pinhole aperture and Si guard slits are shown along with the sample holder, which are all contained in an acrylic enclosure under helium ambiance.

condition. Prepared membranes are caged by a specially designed sample holder to keep the two membranes firmly pressed together. The solution contained between the two membranes is easily preserved for longer than two days at ambient pressure. The diffraction microscope was further equipped with an acrylic enclosure to accommodate helium ambiance, essential both to avoid x rays being scattered by air and to eliminate mechanical stress on the membranes, which would be induced by the pressure difference under vacuum.

We have carried out CDI experiments of fully hydrated biological specimens at BL29XUL of SPring-8. The energy of incident x rays was fixed at 5 keV. Cells mounted between two membranes were inspected using an optical microscope to locate their positions for the x-ray imaging experiments. A 10 μm diameter pinhole aperture was installed at 370 mm upstream of the sample position that accommodates coherent x rays with a constant wave front impinging on the specimen. Si slits were placed to block parasitic scattering from the pinhole and other optical components upstream of the sample as shown in Fig. 1. Incident x-ray flux was monitored using a Si avalanche photodiode. A charge-coupled device (CCD) was placed at 2790 mm downstream of the specimen to record diffraction patterns. The detector is equipped with a direct illumination type Si chip, 1340×1300 pixels with the pixel size of 20 μm chilled by liquid nitrogen (Roper Inc. PI-LCX1300). The detection path, from the sample to the CCD, was kept in vacuum using a 500 nm thick, x-ray transparent Si_3N_4 membrane as an entrance window.

Yeast cells and cyanobacteria were chosen to demonstrate wet CDI. Yeast cells have been imaged extensively with various imaging probes, allowing convenient comparison between wet CDI and established methods [20]. Planktonic cells have weak cell membranes, easily destroyed when dried. However, despite this challenge they contain organelles of significant scientific and technological interest [21]. Imaging them in a fully hydrated state would clearly highlight the merit of wet CDI.

First, we have demonstrated wet CDI by imaging yeast cells. The yeast has been an attractive model system to understand various genetic, biochemical, and morphological aspect of eukaryotes, also frequently imaged by various imaging probes including CDI [22–24]. *Saccharomyces cerevisiae*, budding yeast, were cultured in a 250 ml baffled flask containing 50 ml of YPG growth media (10% yeast extract, 20% Peptone, 20% glucose in deionized water), and incubated at 30 °C for 20 h on a shaking platform at 140 rpm. Yeast cells were dispensed onto the membranes and held stable by gently pressing the two membranes together.

Figure 2(a) displays a speckle pattern obtained from a fully hydrated, unstained, whole yeast cell. The speckle pattern was acquired by accumulating the signals up to a total x-ray dose of 9.6×10^7 Gy, and background signals were subtracted using data measured at a position free from sample. The fringe oscillation reflecting on oval shaped sample morphology is clearly visible from the diffraction pattern. This demonstrates wet CDI's capability to give excellent contrast, even when samples are immersed in solution.

The image was successfully reconstructed in Fig. 2(b), showing internal details with a pixel resolution of 27 nm. We have reconstructed images using the guided hybrid input-output algorithm (GHIO) [25]. The measured

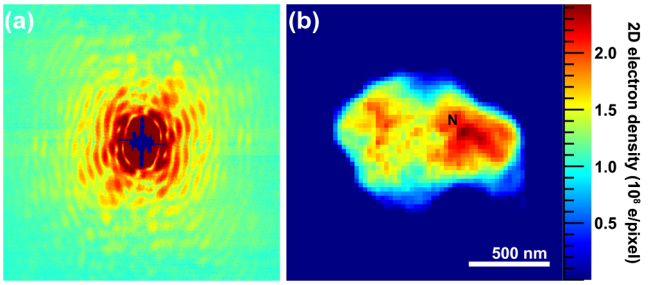

FIG. 2 (color online). (a) Speckle pattern from a fully hydrated, unstained yeast cell. The center of the diffraction pattern in dark blue shows the blocked portion by the x-ray beam stopper, recovered during the phase retrievals. (b) Reconstructed image. The high-density region is likely the nucleus (N) with implied substructures. The projected electron density map is displayed in color with the scale bar to the right.

diffraction pattern was centrosymmetrized with the data size of 1242 × 1242 pixel array. The data were binned by merging a 9 × 9 pixel array into a single pixel, and deconvoluted to recover an exactly oversampled diffraction pattern [26]. The GHIO reconstruction was run with 16 independent reconstructions starting from random phases. Upon finishing 3000 iterations of HIO for each reconstruction, the reconstruction with the lowest R factor, $\sum_{ij}|F_{\mathrm{calc}}(ij) - F_{\mathrm{meas}}(ij)|/\sum_{ij}F_{\mathrm{meas}}(ij)$, was saved from each independent reconstruction; in total 16 images ($\rho^0_{i,\mathrm{min}}$, $i = 1$ to 16) were saved after 16 independent reconstructions. We have chosen the best reconstruction with the lowest R value among all the 16 reconstructions upon completing the 0th generation reconstruction, to best represent the solution of the 0th generation (ρ^0_{best}). Reconstruction was continued, but now starting with a guided image from the previous generation. The guided image is obtained by taking a modular average of the best image from the HIO and the best reconstruction out of all the 16 best images, $\rho^1_i = \sqrt{\rho^0_{i,\mathrm{min}}\rho^0_{\mathrm{best}}}$. The procedure was repeated up to the 9th generation with good convergence among all 16 reconstructions. On finishing the last generation, three images with the lowest R values from 16 reconstructions were averaged to represent the reconstructed image of the diffraction pattern. To verify the fidelity of our reconstruction, we carried out another GHIO reconstruction afresh starting from the random phase. Two images from independent reconstructions are almost identical with more than 97% similarity.

Figure 2(b) displays the obtained image providing a 2D projected electron density, estimated from the intensity at the center pixel of the CCD and the incident photon flux to the sample [15]. The color bar indicates a quantitative measure for the projected electron density. The oval-shaped high-density region may correspond to the nucleus (N). The structure itself further shows localized higher density regions indicating nuclear substructures. The image shares typical morphological features of yeast observed from other work [22–24]. These internal structures are well preserved as can be observed in the lack of contrast degradation.

To further demonstrate the unique merit of wet CDI, we imaged a freshwater cyanobacterium, *Microcystis aeruginosa*, which has many features of scientific and technological importance. In particular, it is a model organism for the study of photosynthesis. Wet CDI holds the potential to advance our understanding on the photosynthetic process with its ability to observe intact thylakoid membranes, the site of the light-dependent reactions of photosynthesis [27]. Further, the carboxysome is the prominent carbon fixation microcompartment. It has attracted much interest recently as a promising candidate for biofuel production [28,29]. Nanoscale imaging of such structures in an intact form expects to provide novel insights. The cell membranes of such cyanobacteria are very fragile, and therefore sensitive to harsh sample treatments. Imaging them under complete hydration is essential for unveiling their substructures intact. This is a major advantage of wet CDI.

The *M. aeruginosa* strain NIES298 was purchased from the National Institute for Environmental Studies, Environmental Agency (Tsukuba, Japan). The strain was maintained and grown with 12 h light illumination and 12 h dark using cold fluorescent lamps (~40 μmol photons $\mathrm{m}^{-2}\,\mathrm{s}^{-1}$) at 30 °C in cytochalasin B medium [21]. Cultured *M. aeruginosa* cells were dispersed onto a membrane together with the medium.

A specimen fully immersed in the buffer media was exposed to x rays up to a radiation dose of 1.3×10^8 Gy in Fig. 3(a). The accumulated speckle pattern was reconstructed in Fig. 3(b), showing the projected electron density, following the same procedures of the GHIO reconstruction described above. Despite the projection being from a whole cell, internal structures are clearly distinguished, and can be compared with the known structures [21]. Distinct high-density spots about 80–100 nm in diameter resemble carboxysomes. Localized spots with a low electron density region imply gas vesicles (G). Layered high-density structures were observed resembling the thylakoid membranes (T) [21].

We compared our result to a transmission electron microscopy image. The TEM image was of the specimen that had been sectioned after embedding in a resin and is shown in Fig. 3(c). The image contrast was enhanced by heavy metal staining, allowing the thylakoid membranes to be

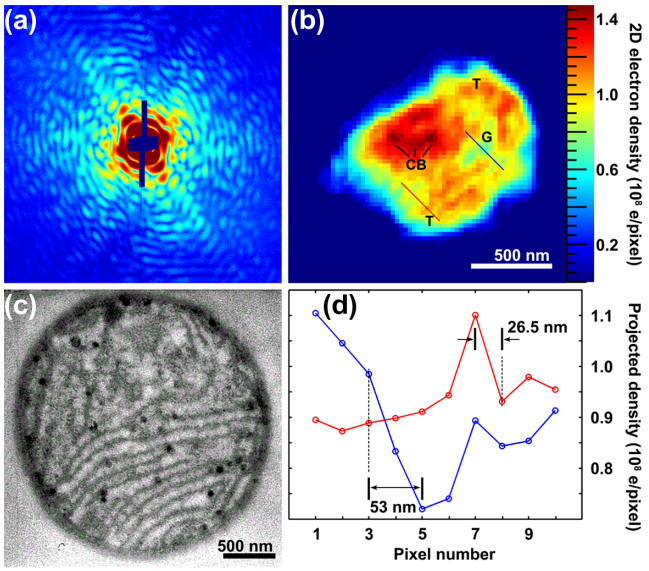

FIG. 3 (color online). (a) Speckle pattern obtained from a hydrated cyanobacterium. (b) Reconstructed image with discernible internal structures labeled as carboxysomes (CB), gas vesicles (G), and thylakoid membranes (T). Projected electron densities are displayed in color with the scale bar to the right. (c) TEM image of sectioned, stained cyanobacetrium. (d) Line plot along the lines in (b) visualizing clear image contrast and 30 nm feature of the thylakoid membrane at better than 50 nm resolution.

seen clearly. Carboxysomes and gas vesicles are not as apparent in this section. The comparison of the two images concludes that wet CDI faithfully provides images of whole, thick cells preserving the internal structures with a well discernible contrast even without any staining. Figure 3(d) shows line cuts, with the blue line around the gas vesicles and the red line across the thylakoid membrane in Fig. 3(b), demonstrating the image contrast and the resolution attained. They visualize the structures with good contrast. In particular, the line cut (red) clearly distinguishes the thylakoid membrane, a 30 nm feature, well demonstrating that we have achieved a resolution better than 55 nm, or 27 nm in the half period [30].

Next we turn to x-ray radiation damage incurred on the specimens. X rays absorbed by specimens generate free radicals resulting in structure deformations via photoelectric ionization, Auger process, etc. The degree of radiation damage varies for different samples in different environments, while being insensitive to the x-ray wavelength [31]. We have carefully monitored the radiation induced sample distortion in wet CDI by recording a series of diffraction patterns with a short-time exposure. The similarity of two speckle patterns $f_i(x, y)$ and $f_j(x, y)$ is evaluated by calculating the cross correlation as $CC_{i,j} = \sum_{x,y} \frac{(f_i(x,y)-\bar{f}_i)(f_j(x,y)-\bar{f}_j)}{\sigma_i \sigma_j}$, where $\bar{f}_i$ and σ_i are the average and standard deviation of the ith speckle pattern, respectively. All of the diffraction patterns remain consistent up to a total x-ray dose of $\sim 1 \times 10^8$ Gy, as shown in Fig. 4(a). It was confirmed that x-ray radiation induced sample damage had no significant effect at this image resolution, similar to previous results with dried or frozen specimens [31–33]. To assess the image resolution, we have calculated the power spectral density (PSD) and phase retrieval transfer function (PRTF) shown in Fig. 4(b). PSD in Fig. 4(b) shows that diffraction signals are not buried by noise down to 40 nm. PRTF measures the resolution-dependent fidelity of image reconstruction by comparing the calculated speckle pattern of the reconstructed image to the actual measured value as $|F_{\mathrm{calc}}(q)|/|F_{\mathrm{meas}}(q)|$. PRTF scores higher than 0.5 for both of the speckle patterns, verifying that the image resolution is better than 40 nm, or 20 nm at half period. This resolution is comparable to the demonstrated value of 25 nm at half period from a recent cryo-CDI experiment, or lower than a factor of 2 compared to the Au labeled, dried sample bioimaging by CDI [23,24]. It should be noted that the image resolution demonstrated here does not yet represent the maximum radiation damage limited attainable values of wet CDI [32,33].

Here, we have introduced wet coherent diffraction microscopy capable of imaging unstained, whole biological specimens immersed completely in solution. Reconstructed images display the specimens' overall morphologies and internal details with outstanding contrast. The spatial resolution presented in this work is not radiation limited yet. With an outstanding contrast of specimens in solution, this newly developed wet CDI expects to be a powerful probe for imaging biological specimens in their native condition. It also holds unbound application to materials systems. Nanoscale imaging of materials' reaction processes in solution is immediately apparent: *in situ* imaging of nucleation and growth of colloidal nanocrystal, liquid-catalyst reactions in ionic battery materials, clay particle agglomeration with the critical importance in petroleum research, etc., [34].

The technique can be readily extended to 3D imaging. 3D tomography can be performed by estimating an acceptable x-ray radiation dose and acquiring each diffraction pattern at $1/N$ reduced dose for the total N number of projections. For usual 3D imaging with 27 projections, for instance, it can be realized at the cost of lowering the maximum achievable resolution by less than a factor of 3 [22,33].

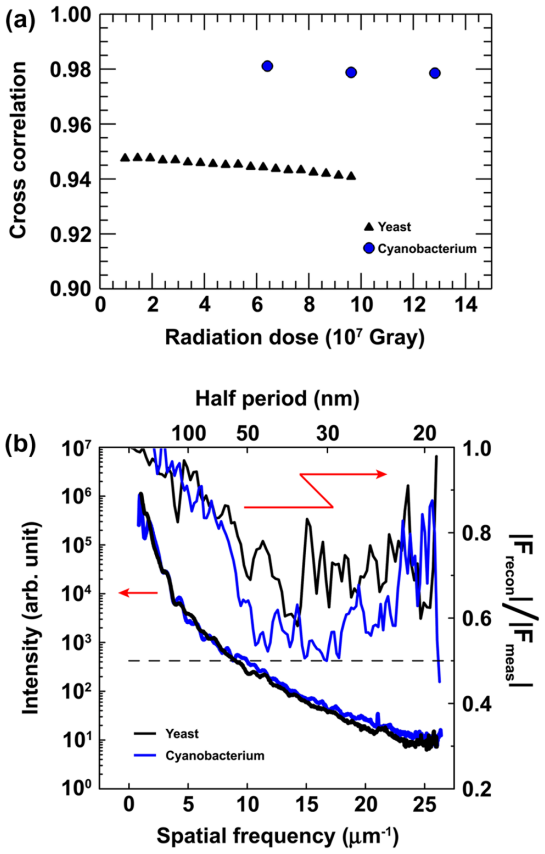

FIG. 4 (color online). (a) Cross correlation function estimated for a series of short time exposed speckle patterns from a yeast (triangle) and cyanobacterium (circle). Speckle patterns remain consistent up to the total exposure of $\sim 1 \times 10^8$ Gy. (b) Power spectral density (PSD, left axis) and phase retrieval transfer function (PRTF, right axis) of the accumulated speckle patterns of the yeast (black) and cyanobacterium (blue). Both of PSD and PRTF manifest that signals from the sample extend a spatial resolution better than 40 nm, or 20 nm in half period, with reliable phase retrieval.

We want to emphasize that wet CDI is a cross-platform imaging technique, which can be employed at any coherent source. In x rays, there has been remarkable progress in hosting intense synchrotron x-ray sources, ultrabright and short-pulsed x-ray free electron lasers (XFEL), and tabletop soft x-ray lasers with concentrated interest in establishing versatile nanoscale imaging probes. Wet CDI will provide significant impact to unravel ultrastructures of intact biological specimens and reactive materials nanostructures by best utilizing these sources. Cryocooling of biological specimens has been introduced in CDI [23,35]. The cryo-CDI technique may find applications in high-resolution imaging of biological specimens but in static states. Wet CDI expects to facilitate high-resolution dynamic imaging by addition of a chemical reactant, enzyme, virus, etc., to the buffer solution surrounding living cells, further deepening our understanding of the processes taking place in living systems. The benefits of adaptation to XFEL are immediate with the potential of no radiation damage to limited live cell imaging by taking advantage of ultrashort x-ray pulses.

This research was supported by RIKEN and in part by MEXT. The authors thank D. Choi for providing the yeast cell line, and H. Shimada for his help on the illustration. C. S. thanks K.-B. Lee for the support of the project through D. N. This work is supported in part by NRF through the NCRC (Grant No. R15-2008-006-00000-0).

*To whom correspondence should be addressed.
cysong@spring8.or.jp

[1] J. Pawley, J Biomed. Opt. **13**, 029902 (2008).
[2] A. Cavalier, D. Spehner, and B. M. Humbel, *Handbook of Cryo-Preparation Methods for Electron Microscopy* (CRC Press, Boca Raton, 2009).
[3] S. A. Jones, S.-H. Shim, J. He, and X. Zhuang, Nat. Methods **8**, 499 (2011).
[4] E. Betzig, G. H. Patterson, R. Sougrat, O. W. Lindwasser, S. Olenych, J. S. Bonifacino, M. W. Davidson, J. Lippincott-Schwartz, and H. F. Hess, Science **313**, 1642 (2006).
[5] S. W. Hell, Science **316**, 1153 (2007).
[6] S. T. Hess, T. P. K. Girirajan, and M. D. Mason, Biophys. J. **91**, 4258 (2006).
[7] D. F. Parsons, Science **186**, 407 (1974).
[8] N. d. Jonge, D. B. Peckys, G. J. Kremers, and D. W. Piston, Proc. Natl. Acad. Sci. U.S.A. **106**, 2159 (2009).
[9] J. Kirz, C. Jacobsen, and M. Howells, Q. Rev. Biophys. **28**, 33 (1995).
[10] G. Poletti *et al.*, Eur. Phys. J. D **30**, 235 (2004).
[11] A. Momose, Jpn. J. Appl. Phys. **44**, 6355 (2005).
[12] J. Miao, R. L. Sandberg, and C. Song, IEEE J. Sel. Top. Quantum Electron. **18**, 399 (2012).
[13] H. N. Chapman and K. A. Nugent, Nat. Photonics **4**, 833 (2010).
[14] M. A. Pfeifer, G. J. Williams, I. A. Vartanyants, R. Harder, and I. K. Robinson, Nature (London) **442**, 63 (2006).
[15] C. Song, H. Jiang, A. Mancuso, B. Amirbekian, L. Peng, R. Sun, S. Shah, Z. Zhou, T. Ishikawa, and J. Miao, Phys. Rev. Lett. **101**, 158101 (2008).
[16] M. M. Seibert *et al.*, Nature (London) **470**, 78 (2011).
[17] S. Williams, X. Zhang, C. Jacobsen, J. Kirz, S. Lindaas, J. Van't Hof, and S. S. Lamm, J. Microsc. **170**, 155 (1993).
[18] A. C. Cefalas, P. Argitis, Z. Kollia, E. Sarantopoulou, T. W. Ford, A. D. Stead, A. Marranca, C. N. Danson, J. Knott, and D. Neely, Appl. Phys. Lett. **72**, 3258 (1998).
[19] S. Bollanti *et al.*, J. X-Ray Sci. Technol. **5**, 261 (1995).
[20] D. Batani *et al.*, Phy. Med. **14**, 151 (1998).
[21] T. Yoshida, Y. Takashima, Y. Tomaru, Y. Shirai, Y. Takao, S. Hiroishi, and K. Nagasaki, Appl. Environ. Microbiol. **72**, 1239 (2006).
[22] H. Jiang *et al.*, Proc. Natl. Acad. Sci. U.S.A. **107**, 11234 (2010).
[23] X. Huang *et al.*, Phys. Rev. Lett. **103**, 198101 (2009).
[24] J. Nelson, X. Huang, J. Steinbrener, D. Shapiro, J. Kirz, S. Marchesini, A. M. Neiman, J. J. Turner, and C. Jacobsen, Proc. Natl. Acad. Sci. U.S.A. **107**, 7235 (2010).
[25] C.-C. Chen, J. Miao, C. Wang, and T. Lee, Phys. Rev. B **76**, 064113 (2007).
[26] C. Song, D. Ramunno-Johnson, Y. Nishino, Y. Kohmura, T. Ishikawa, C.-C. Chen, T.-K. Lee, and J. Miao, Phys. Rev. B **75**, 012102 (2007).
[27] A. M. Collins, M. Liberton, H. D. T. Jones, O. F. Garcia, H. B. Pakrasi, and J. A. Timlin, Plant Physiol. **158**, 1600 (2012).
[28] T. O. Yeates, C. A. Kerfeld, S. Heinhorst, G. C. Cannon, and J. M. Shively, Nat. Rev. Microbiol. **6**, 681 (2008).
[29] D. F. Savage, B. Afonso, A. H. Chen, and P. A. Silver, Science **327**, 1258 (2010).
[30] M. Liberton, L. E. Page, W. B. O'Dell, H. O'Neill, E. Mamontov, V. S. Urban, and H. B. Pakrasi, J. Biol. Chem. **288**, 3632 (2013).
[31] R. Henderson, Q. Rev. Biophys. **28**, 171 (1995).
[32] M. R. Howells *et al.*, J. Electron Spectrosc. Relat. Phenom. **170**, 4 (2009).
[33] Q. Shen, I. Bazarov, and P. Thibault, J. Synchrotron Radiat. **11**, 432 (2004).
[34] P. Simon and Y. Gogotsi, Nat. Mater. **7**, 845 (2008).
[35] E. Lima, L. Wiegart, P. Pernot, M. Howells, J. Timmins, F. Zontone, and A. Madsen, Phys. Rev. Lett. **103**, 198102 (2009).